



**Showcasing research by the group of Prof. Angiolina Comotti  
at the Department of Materials Science at the University of  
Milano Bicocca.**

#### Porous dipeptide crystals as volatile-drug vessels

We show the activity of porous materials of natural origin in capturing and releasing volatile anesthetics. A multitechnique approach allowed us to highlight the accommodation of the fluorinated molecules in the confined spaces, mimicking their arrangement in the biological receptors.

#### As featured in:



See Angiolina Comotti *et al.*,  
*Chem. Commun.*, 2018, **54**, 148.



[rsc.li/chemcomm](http://rsc.li/chemcomm)

Registered charity number: 207890



## Porous dipeptide crystals as volatile-drug vessels†

S. Bracco,  D. Asnaghi,  M. Negroni,  P. Sozzani  and A. Comotti  \*Cite this: *Chem. Commun.*, 2018, 54, 148Received 19th August 2017,  
Accepted 25th October 2017

DOI: 10.1039/c7cc06534e

rsc.li/chemcomm

**Porous crystalline dipeptides absorb, reversibly from the gas phase, a series of volatile fluorinated ethers in use as anesthetics. Their vapor pressure was considerably reduced, with favorable guest capture and release. Variable channel sizes were customized for selective sorption and pressure thresholds were observed in the narrowest pores.  $^1\text{H}$ ,  $^{13}\text{C}$  and  $^{19}\text{F}$  MAS NMR coupled with *ab initio* conformational analysis and grand canonical Monte Carlo simulations highlight the guest loading and arrangement adopted in the congruent nanochannels, suggesting how the anesthetics can accommodate in biochemical receptors.**

In recent years intense development in the field of porous materials with nanometric and sub-nanometric pore dimensions has enabled the confinement and release of gases and volatile molecules with high efficiency.<sup>1</sup> Indeed, in addition to conventional inorganic materials, such as zeolites,<sup>2</sup> hybrid materials and fully organic frameworks have been proposed.<sup>3</sup> Thus, the nature of the bonds sustaining the structures was extended to metal-organic, covalent-organic bonds as well as to soft supramolecular interactions, which produce porous materials denominated hydrogen bonded organic frameworks (HOFs), supramolecular organic frameworks (SOFs) and porous molecular crystals (PMCs).<sup>4</sup> The easy self-assembly from their molecular constituents as well as the processability in solution make them particularly attractive. In this context, biological molecules, especially dipeptides composed by proteinogenic amino-acids, are able to self-assemble into porous architectures and have been proposed as absorptive materials.<sup>5</sup> Such dipeptides are outstanding for their large variety of available channels. Supramolecular interactions as stable as charge assisted hydrogen bonding between ammonium and carboxylate end-groups support the porous structure. They are biodegradable and thus environmentally friendly, as opposed to the majority of porous materials. However, their use as volatile drug vessels has never been explored.

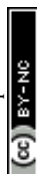
Halogenated ethers and alkanes have extensive applications in general anesthesia, although there are still difficulties in their storage and delivery without dispersion into the environment.<sup>6</sup> Halothane, enflurane, desflurane and isoflurane, and the non-halogenated diethyl ether, are among the most commonly used substances as anesthetics. These compounds, administered by inhalation, interact with GABA<sub>A</sub> receptors in synaptic membranes and cause a reversible loss of consciousness.<sup>7</sup> Moreover, most of them belong to the category of chlorofluorocarbon ethers (CFCs) and thus represent a constant danger for the environment.<sup>8</sup>

The use of biocompatible peptides in various association states make them suitable as drug delivery systems for hydrophobic drugs.<sup>9</sup> However, crystalline porous dipeptides have not yet been exploited for hosting/releasing volatile drugs, although they are particularly intriguing for the subnanometric size of the available spaces. The reduction of the vapor pressure of commonly-used volatile anesthetics upon nanoconfinement may give rise to practical advantages in handling and storage,<sup>10</sup> as well as in delivery for controlled administration.<sup>9</sup> Moreover, the use of nanocrystals as hydrophobic-drug carriers may be attractive for parenteral or oral administration, thanks to the increased solubility and, thus, bio-availability. Herein we present adsorption/desorption isotherms of ultra-microporous dipeptide crystals and spectroscopic evidences for guest-anesthetic arrangement in the nanochannels (Fig. 1).

In particular, we investigated porous dipeptides L-valyl-L-alanine (VA), L-alanyl-L-isoleucine (AI), L-valyl-L-valine (VV), L-isoleucyl-L-valine (IV) and L-isoleucyl-L-alanine (IA), whose hexagonal crystal structures (space group *P6<sub>1</sub>*) exhibit one-dimensional channels.<sup>5</sup> The family of volatile halogenated ethers and alkanes was chosen as probing guests, given the high vapour pressure already at 273 K. Pores with tailored cross-sections from 5.3 Å to 3.5 Å, as modulated by aliphatic groups lining the inner surface of the walls, offer a great versatility for studying vapour absorptive properties, especially, selectivity and capacity towards these guests. Indeed, pore size plays a key role in the selective recognition of the anesthetics: dipeptide crystals with channels larger than 4 Å such as VA, AI and VV efficiently absorb the guests whilst IA and IV with pore sizes of about 3.5 Å exclude the anesthetics.

Department of Materials Science, University of Milano Bicocca and INSTM Consortium, via R. Cozzi 55, 20125, Milano, Italy.  
E-mail: angiolina.comotti@unimib.it

† Electronic supplementary information (ESI) available: Experimental part, PXRD,  $^{13}\text{C}$ ,  $^1\text{H}$  and  $^{19}\text{F}$  MAS NMR spectroscopy, conformational analysis. See DOI: 10.1039/c7cc06534e



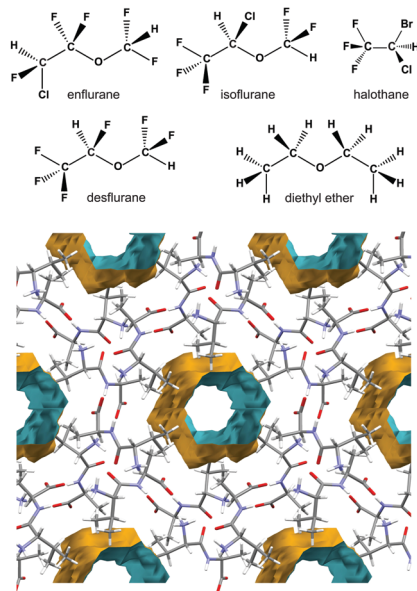


Fig. 1 Chemical structures of the halogenated ethers used as guests (above); portion of the crystal structure of L-valyl-L-alanine (VA) along the channels axis (below).

The vapor isotherms are reported in Fig. 2. The adsorption in VA channels ( $d = 5.1\text{--}5.3\text{ \AA}$ , as calculated by an exploring sphere of  $2\text{ \AA}$  radius)<sup>11</sup> exhibited Langmuir-type profiles for all the halogenated guests showing maximum absorption values of  $170\text{--}200\text{ mmol mol}^{-1}$  at  $273\text{ K}$  and  $80\text{--}100\text{ Torr}$ , which correspond to a virtually complete loading of available volume and more than 20% by weight. The unit cell parameters of the samples upon loading remain substantially unaltered, indicating the zeolitic behavior of the molecular crystalline material. Langmuir-type isotherms for enflurane are also shown in the smaller channels of AI ( $4.7\text{--}5.0\text{ \AA}$ ) and VV ( $4.0\text{--}4.2\text{ \AA}$ ) owing to the limited steric requirements of the chlorine on the terminal methyl group, which allows easy adjustment in the channels. On the contrary, the isotherms of the isoflurane isomer bearing the chlorine substituent on the methylene group and halothane (containing F, Cl and Br halogens) in VV do not follow a Langmuir profile, this different behavior is particularly accentuated in the case of halothane. In fact, in the channels of VV, halothane isotherms exhibited a minimal adsorption at low pressures followed by an increased uptake above  $10\text{ Torr}$ . Thus, at low pressures a selective absorption of enflurane with respect to halothane is exhibited. This behavior is fully reproducible over a few cycles and can be attributed to the flexibility of the structure that expanded upon crossing a pressure threshold. On the contrary, in IA and IV nanochannels with cross-sections of about  $3.5\text{ \AA}$  the halogenated molecules are excluded for their exceeding steric encumbrance. Interestingly, dipeptides containing the same aminoacids, alanine and isoleucine, in opposite sequences, AI and IA, generate different cross-sections (from  $4.7\text{--}5.0\text{ \AA}$  to  $3.5\text{ \AA}$ , respectively), that can differentiate the adsorption properties of the same guest (Fig. 2). Desflurane, bearing exclusively fluorine atoms as halogens and exhibiting the highest volatility (b.p. =  $23\text{ }^{\circ}\text{C}$ ), shows in all dipeptides modest absorption values at  $273\text{ K}$

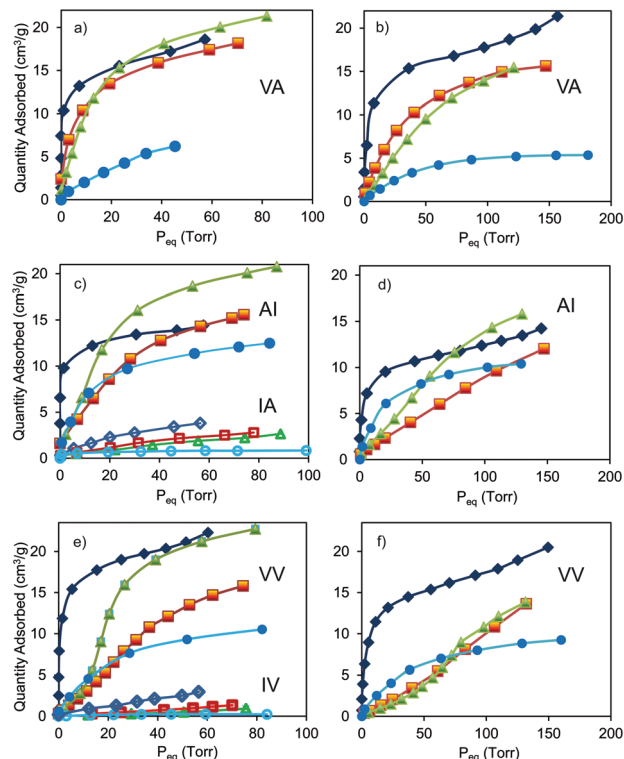


Fig. 2 Anesthetics adsorption isotherms: in VA at  $273\text{ K}$  (a) and at  $298\text{ K}$  (b); in AI and IA at  $273\text{ K}$  (c) and in AI at  $298\text{ K}$  (d); in VV and IV at  $273\text{ K}$  (e) and in VV at  $298\text{ K}$  (f). Enflurane (blue diamond), isoflurane (orange square), halothane (green triangle) and desflurane (light blue circle). In IA and IV the labels are empty.

whilst diethylether is absorbed with high efficiency in the hydrocarbon environment (ESI<sup>†</sup>). Desorption branches show complete reversibility of the isotherms and no hysteresis, indicating possible reuse of dipeptides without regeneration (ESI<sup>†</sup>).

From adsorption isotherms at various temperature, we evaluated the isosteric heats of adsorption (see ESI<sup>†</sup>) by applying the Clausius–Clapeyron equation. We found out values in the range of  $35\text{--}50\text{ kJ mol}^{-1}$ , which demonstrate the strong affinity between the dipeptide hosts and the guests owing to multiple interactions installed within the narrow channels. These adsorption energies are comparable to the highest values reported for adsorbed anesthetics in porous materials.<sup>10c</sup>

Fast magic angle spinning  $^1\text{H}$  NMR spectra provided direct evidence of the inclusion of the anesthetics in the crystalline channels of VA, AI and VV upon sorption from the gas phase (Fig. 3) (see ESI<sup>†</sup>). An interesting feature is the upfield shift ( $\delta = -0.2\text{ ppm}$ ) of included halogenated ethers with respect to the pure compounds, owing to the magnetic susceptibility generated by the dipeptide environment.<sup>12</sup> Specifically, a sample with an excess of enflurane in VA allowed us to distinguish the signals of free and included enflurane. The signals of the included halogenated molecules have a linewidth wider than that of free molecules owing to stronger  $^1\text{H}$  homonuclear coupling, indicating that guest molecules undergo restricted motion. Quantitative analysis of the amount of included anesthetics with respect to the dipeptide hosts allowed us to measure the maximum loading



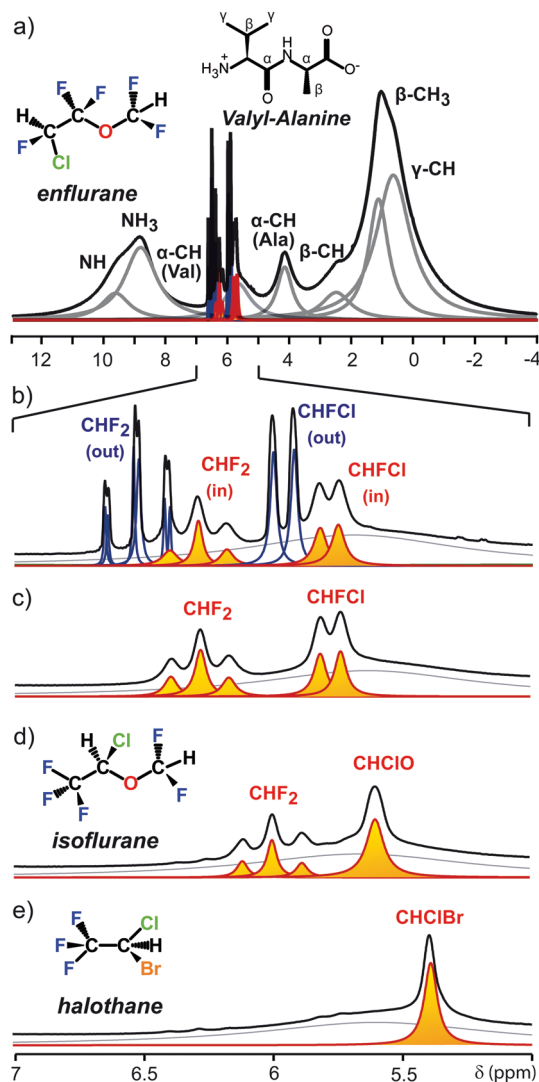


**Fig. 3** 600  $^1\text{H}$  fast-MAS NMR (35 kHz spinning speed): (a) VA with enflurane both inside and outside the nanochannels; (b) enlargement of the above spectrum in the 5–7 ppm range.  $^1\text{H}$  spectra (5–7 ppm range) of VA fully loaded with (c) enflurane, (d) isoflurane and (e) halothane. The signals of halogenated ethers confined in the nanochannels and in the bulk are highlighted in orange and blue, respectively.

of the channels. Enflurane, isoflurane and halothane in VA were found to be 0.19, 0.16 and 0.19 mol mol $^{-1}$ , respectively, in agreement with the amount measured from adsorption isotherms at 273 K (0.18, 0.16 and 0.19 mol mol $^{-1}$ , respectively).

However, the conformational arrangement of anesthetics in confined spaces has never been investigated.  $^{19}\text{F}$  MAS NMR spectra of isoflurane in all the dipeptides show a dramatic change with respect to the spectra in the liquid state (Fig. 4). Indeed, the  $^{19}\text{F}$  NMR spectra of isoflurane confined in VA showed two distinct triplets separated by about 5.3 ppm for the two fluorine nuclei of the  $\text{CHF}_2$  group (Fig. 4c), in contrast to a single multiplet recorded for pure isoflurane in the bulk wherein fast exchange among conformers occurs (Fig. 4b). Such large separation must be ascribed to the conformational arrangement of the two fluorine atoms and the  $\gamma$ -gauche effect

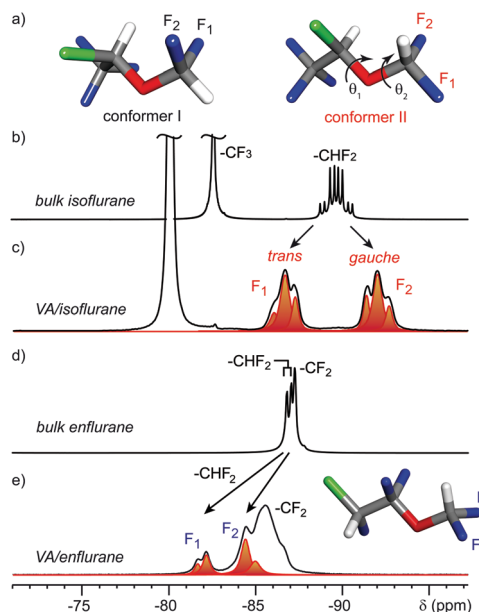


**Fig. 4** (a) The two conformational minima of isoflurane: conformer I and II with C–C–O–C of 139° and of 166°, respectively.  $^{19}\text{F}$  MAS NMR spectra of (b) isoflurane on celite, (c) isoflurane in VA, (d) enflurane on celite, (e) enflurane in VA.

that produces an upfield shift of 5 ppm when the observed nucleus changes from a *trans* to a *gauche* conformation.<sup>13</sup>

A theoretical study allowed us to establish the most stable conformers of isoflurane. We explored the dihedral angles  $\theta_1$  and  $\theta_2$  (C–C–O–C and F<sub>1</sub>–C–O–C, respectively) and observed the stability of two conformational minima in the energy map with values as close as  $\Delta = 0.5$  kcal mol $^{-1}$  (Fig. 4a). In conformer I, the F–C–O–C dihedral angles for F<sub>1</sub> and F<sub>2</sub> are  $-63^\circ$  and  $58^\circ$  (*i.e.* both in *gauche* conformation); on the contrary in conformer II the F<sub>1</sub>–C–O–C and F<sub>2</sub>–C–O–C dihedral angles are  $177^\circ$  and  $-62^\circ$ , respectively (*i.e.* F<sub>1</sub> in *trans* and F<sub>2</sub> in *gauche* conformations).<sup>14</sup> The experimental spectrum clearly indicates that the conformer II (with the torsional angle  $\theta_2$  setting F<sub>1</sub> in *trans* and F<sub>2</sub> in *gauche* conformation) provides the only feasible arrangement of isoflurane confined in the narrow dipeptide channels: in fact, the behavior of included isoflurane is common to all the observed dipeptide crystals, such as AI and VV (Fig. S25, ESI $^\dagger$ ). Indeed, the lateral steric encumbrance is reduced in conformer II because at least one of the two fluorine atoms is set in the more elongated *trans* arrangement, whereas in conformer I both fluorines protrude laterally in *gauche* arrangement. Conformer II also displayed a  $\theta_1$  torsional angle close to a *trans* arrangement, setting the main chain in the most elongated conformation.  $^{13}\text{C}$  CP MAS spectra decoupled from  $^1\text{H}$  or  $^{19}\text{F}$  (see Fig. S26 and S28, ESI $^\dagger$ ) are in agreement with the stretched conformation preferred for the steric requirements imposed by the crystalline channels. In the case of enflurane, a different behavior is observed for the  $\text{CHF}_2$  group. Actually, the two fluorine nuclei resonate downfield with respect to those of the structural isomer isoflurane (Fig. 4e). This is due to the conformation of the two fluorine atoms, which are set at F–C–O–C dihedral angles of  $-105^\circ$  and  $135^\circ$  (ESI $^\dagger$ ) and



thus do not undergo  $\gamma$ -gauche effect when enflurane is included in the VA channels. The GCMC simulations of enflurane and isoflurane isotherms in VA show that the energetically stable conformers occupy the channels with a maximum loading corresponding to that of the experimental isotherms and the guests are not periodically distributed along the channels.

Dynamic light scattering analysis of a suspension of crystals proved that their particle size falls in the nanometric range with a distribution centered at about 30 nm. This evidence enforces the perspectives for the use of dipeptides in nanomedicine, because this particle size is suitable for blood stream transport and cell internalization.

In conclusion, dipeptide crystals, with their ultra-micropores, offer suitable room for hosting anesthetic molecules and tuning their volatility. The diversity in the size and shape of the space available for the guests in the numerous dipeptide structures allowed us to select the most appropriate dipeptide crystals for specific guests and show the remarkable selectivity. The guests included in the dipeptide crystals were detected by  $^{13}\text{C}$ ,  $^{19}\text{F}$  and fast- $^1\text{H}$  MAS NMR spectroscopy, which provided a detailed analysis of the arrangement of the guest molecules in the cavities and the amount of loaded anesthetics, in agreement with the adsorption isotherms. This investigation may shed light on the way volatile anesthetics adapt to variable-size subnanometric channels, mimicking biological receptors. Moreover, the biodegradability and biocompatibility of nanoporous dipeptide materials encourages their use in biomedical applications.

Cariplo Foundation 2016, PRIN 2015-CTEBBA and INSTM Consortium IN-RL14-2016 are acknowledged for financial support. The authors would like to thank D. Piga for helpful discussion.

## Conflicts of interest

There are no conflicts to declare.

## Notes and references

- 1 S. Kitagawa, *Angew. Chem., Int. Ed.*, 2015, **54**, 10686.
- 2 D. W. Breck, *Zeolite Molecular Sieves. Structure, Chemistry and Use*, Wiley, New York, 1974, p. 593.
- 3 (a) H.-C. Zhou, J. R. Long and O. M. Yaghi, *Chem. Rev.*, 2012, **112**, 673; (b) S. Das, P. Heasman, T. Ben and S. Qiu, *Chem. Rev.*, 2017, **117**, 1515; (c) Z. Zhang and M. J. Zaworotko, *Chem. Soc. Rev.*, 2014, **43**, 5444; (d) N. Huang, P. Wang and D. Jiang, *Nat. Rev. Mater.*, 2016, **1**, 1; (e) P. J. Waller, F. Gandara and O. M. Yaghi, *Acc. Chem. Res.*, 2015, **48**, 3053.
- 4 (a) H. Wang, B. Li, H. Wu, T.-L. Hu, Z. Yao, W. Zhou, S. Xiang and B. Chen, *J. Am. Chem. Soc.*, 2015, **137**, 9963; (b) S. A. Dalrymple and G. K. H. Shimizu, *J. Am. Chem. Soc.*, 2007, **129**, 12114; (c) N. B. McKewon, *J. Mater. Chem.*, 2010, **20**, 10588; (d) P. Sozzani, S. Bracco, A. Comotti, L. Ferretti and R. Simonutti, *Angew. Chem., Int. Ed.*, 2005, **44**, 1816; (e) M. Baroncini, S. d'Agostino, G. Bergamini, P. Ceroni, A. Comotti, P. Sozzani, I. Bassanetti, F. Grepioni, T. M. Hernandez, S. Silvi, M. Venturi and A. Credi, *Nat. Chem.*, 2015, **7**, 634; (f) A. Comotti, S. Bracco, A. Yamamoto, M. Beretta, T. Hirukawa, N. Tohnai, M. Miyata and P. Sozzani, *J. Am. Chem. Soc.*, 2014, **136**, 618; (g) A. Pulido, L. Chen, T. Kaczorowski, D. Holden, M. A. Little, S. Y. Chong, B. J. Slater, D. P. McMahon, B. Bonillo, C. J. Stackhouse, A. Stephenson, C. M. Kane, R. Clowes, T. Hasell, A. I. Cooper and G. M. Day, *Nature*, 2017, **543**, 657; (h) W. Yang, A. Greenaway, X. Lin, R. Matsuda, A. J. Blake, C. Wilson, W. Lewis, P. Hubberstey, S. Kitagawa, N. R. Champness and M. Schröder, *J. Am. Chem. Soc.*, 2010, **132**, 14457; (i) M. Mastalerz and I. M. Oppel, *Angew. Chem., Int. Ed.*, 2012, **51**, 5252; (j) R. S. Patil, D. Banerjee, C. Zhang, P. K. Thallapally and J. L. Atwood, *Angew. Chem., Int. Ed.*, 2016, **55**, 4523; (k) V. N. Yadav, A. Comotti, P. Sozzani, S. Bracco, T. Bonge-Hansen, M. Hennum and C.-H. Gorbitz, *Angew. Chem., Int. Ed.*, 2015, **54**, 15684; (l) Y. Liu, C. Hu, A. Comotti and M. D. Ward, *Science*, 2011, **333**, 436; (m) I. Bassanetti, F. Mezzadri, A. Comotti, P. Sozzani, M. Gennari, G. Calestani and L. Marchio, *J. Am. Chem. Soc.*, 2012, **134**, 9142.
- 5 (a) C. H. Gorbitz and E. Gundensen, *Acta Crystallogr., Sect. C: Cryst. Struct. Commun.*, 1996, **52**, 1764; (b) C. H. Gorbitz, *Chem. – Eur. J.*, 2007, **13**, 1022; (c) A. Comotti, S. Bracco, G. Distefano and P. Sozzani, *Chem. Commun.*, 2009, 284; (d) A. Comotti, A. Fraccarollo, S. Bracco, M. Beretta, G. Distefano, M. Cossi, L. Marchese, C. Riccardi and P. Sozzani, *CrystEngComm*, 2013, **15**, 1503; (e) D. V. Soldatov, I. L. Moudrakoski and J. A. Ripmeester, *J. Am. Chem. Soc.*, 2006, **128**, 6737; (f) R. V. Alfonso, J. Durão, A. Mendes, A. M. Damas and L. Gales, *Angew. Chem., Int. Ed.*, 2010, **49**, 3034; (g) G. Distefano, A. Comotti, S. Bracco, M. Beretta and P. Sozzani, *Angew. Chem., Int. Ed.*, 2012, **51**, 9258; (h) S. Lim, H. Kim, N. Selvapalam, K.-J. Kim, S. J. Cho, G. Seo and K. Kim, *Angew. Chem., Int. Ed.*, 2008, **47**, 3352.
- 6 J. F. Hendrick, E. I. Eger, J. M. Sonner and S. L. Shafer, *Anesth. Analg.*, 2008, **107**, 494.
- 7 (a) P. S. Garcia, S. E. Kolesky and A. Jenkins, *Curr. Neuropharmacol.*, 2010, **8**, 2; (b) P. S. Miller and A. Radu Aricescu, *Nature*, 2014, **512**, 270.
- 8 (a) S. M. Ryan and N. J. Claus, *Anesth. Analg.*, 2010, **111**, 92; (b) S. Y. Jeffrey and J. White, *Anesth. Prog.*, 2012, **59**, 154; (c) J. Sherman, C. Le, V. Lamers and M. Eckelman, *Anesth. Analg.*, 2012, **114**, 108; (d) M. P. Sulbaek Andersen, S. P. Sander, O. J. Nielsen, D. S. Wagner, T. J. Sanford Jr and T. J. Wallington, *Br. J. Anaesth.*, 2010, **6**, 760.
- 9 (a) Y. Chen, C. Tang, J. Zhang, M. Gong, B. Su and F. Qiu, *Int. J. Nanomed.*, 2015, **10**, 847; (b) M. Vallet-Regi, F. Balas and D. Arcos, *Angew. Chem., Int. Ed.*, 2007, **46**, 7548.
- 10 (a) B. F. Abrahams, A. D. Dharma, P. S. Donnelly, T. A. Hudson, C. J. Kepert, R. Robson, P. D. Southon and K. F. White, *Chem. – Eur. J.*, 2017, **23**, 7871; (b) T. H. Chen, W. Kaveevivitchai, A. J. Jacobson and O. S. Miljanic, *Chem. Commun.*, 2015, **51**, 14096; (c) N. Gargiulo, A. Peluso, P. Aprea, Y. Hua, D. Filipovi, D. Caputo and M. Eic, *RSC Adv.*, 2014, **4**, 49478.
- 11 The average diameter ( $d$ ) of the dipeptide channels was established by the exploration of a  $2\text{ \AA}$  sphere of available volume ( $V$ ) and considering a cylinder of height equal to  $c$  unit cell parameter, according to the formula  $d = 2(V/c\pi)^{1/2}$ .
- 12 (a) S. Brown, *Prog. Nucl. Magn. Reson. Spectrosc.*, 2007, **50**, 199; (b) S. Bracco, A. Comotti, P. Valsesia, M. Beretta and P. Sozzani, *CrystEngComm*, 2010, **12**, 2318; (c) S. Bracco, A. Comotti, L. Ferretti and P. Sozzani, *J. Am. Chem. Soc.*, 2011, **133**, 8982; (d) P. A. Williams, C. E. Hughes, J. Martin, E. Courvoisier, A. B. M. Buanz, S. Gaisford and K. D. M. Harris, *J. Phys. Chem. C*, 2016, **120**, 9385.
- 13 D. G. Gorenstein, *J. Am. Chem. Soc.*, 1977, **99**, 2254.
- 14 (a) A. Lesarri, A. Vega-Toribio, R. D. Suenram, D. J. Brugh, D. Nori-Shargh, J. E. Boggsd and J.-U. Grabow, *Phys. Chem. Chem. Phys.*, 2011, **13**, 6610; (b) A. Pfeiffer, H.-G. Mack and H. Oberhammer, *J. Am. Chem. Soc.*, 1998, **120**, 6384.

